Global Change Biology (2008) **14**, 1008–1017, doi: 10.1111/j.1365-2486.2008.01550.x

Scaling-up knowledge of growing-season net ecosystem exchange for long-term assessment of North Dakota grasslands under the Conservation Reserve Program

REBECCA L. PHILLIPS* and OFER BEERI†

USDA-ARS, Northern Great Plains Research Lab, Box 459, Mandan, ND 58554, †University of North Dakota, John D. Odegard School of Aerospace Sciences, Department of Space Studies, Grand Forks, ND 58202-9008

Abstract

Scaling-up knowledge of land-atmosphere net ecosystem exchange (NEE) from a single experimental site to numerous perennial grass fields in the Northern Great Plains (NGP) requires appropriate scaling protocols. We addressed this problem using synoptic data available from the Landsat sensor for 10 growing seasons (April 15 to September 30) over a North Dakota field-site, where we continuously measured CO_2 exchange using a Bowen Ratio Energy Balance (BREB) system. NEE observed during the growing season at our field-site from 1997 to 2006 vacillated with drought and deluge, with net carbon (C) losses to the atmosphere in 2006. We used stepwise linear regression with 10 years of Landsat and NEE data to construct and validate a model for estimating grassland growing-season NEE from field to landscape scales. Eighty-nine percent of the variability in NEE was explained by year, live biomass, carbon : nitrogen ratio, day of image acquisition, and annual precipitation. We then applied this model on 20 620 ha of North Dakota perennial grass fields enrolled in the Conservation Reserve Program (CRP), including 1272 fields east of the Missouri River and 165 fields west-river. Growing-season NEE for individual CRP fields was highly variable from 1997 to 2006, ranging from -366 to 692 g C m^{-2} growing season^{-1}. Mean annual growing-season fluxes over 10 years for CRP fields located east-river and west-river were 317 g C m^{-2} growing season^{-1} and 239 g C m^{-2} growing season^{-1}, respectively. Average cumulative growing-season NEE modeled for fields east- and west-river diverged from one another in 2002–2006, when west-river fields received $<70\%$ of the long-term annual average precipitation during these years. Results indicate assessment of conservation practices on grassland CO_2 exchange during the growing season can be remotely estimated at field and landscape scales under variable environmental conditions and should be followed up with similar, spatially explicit investigations of NEE during the dormant season.

Keywords: assessment, ASTER, biomass, C/N ratio, carbon, climate, Landsat, monitoring, NEE

Received 1 August 2007; revised version received 22 October 2007 and accepted 2 November 2007

Introduction

Quantification of how agricultural management practices influence growing-season net ecosystem exchange (NEE) in the Northern Great Plains (NGP) is limited by the number of long-term measurement sites (Verburg *et al*., 2004). Lack of data, particularly data spanning a wide range of environmental conditions, restrains knowledge of how NEE changes with land management (Suyker *et al*., 2003; Wylie *et al*., 2007). Net CO_2-C uptake may be greater for annual crop fields converted to perennial grasses under the Conservation Reserve Program (CRP) because these fields are not mechanically disturbed by tillage or chemically amended with fertilizers that release additional greenhouse gases (Robertson *et al*., 2000). However, effects of conservation on plant mediated exchange of C between the land and atmosphere will likely vary (with plant properties and processes) over time and space, calling for temporally and spatially explicit biological information. Moderate-to-high resolution optical data can be used to model live biomass (LB) and canopy carbon : nitrogen ratio (CN) for NGP grasslands (Beeri *et al*., 2007b). Synoptic tools for delineating plant

Correspondence: Rebecca L. Phillips, tel. +701 667 3002, fax +701 667 3054, e-mail: rebecca.phillips@ars.usda.gov

properties offer potential vehicles for 'scaling up' current knowledge of grassland growing-season NEE necessary to address landscape-scale questions.

Grasslands in North Dakota (ND) are highly influenced by annual precipitation, with productivity patterns following an east-to-west precipitation gradient across the state (Rogler & Haas, 1946). Production is also affected by the timing of precipitation events (Knapp *et al*., 2002). Grassland NEE data collected during 6 normal-to-high rainfall years at Mandan, ND, indicated growing-season NEE varied from 500 to 1500 kg C ha^{-1} (Frank, 2004). However, growing-season NEE during low precipitation years has not been reported for ND grasslands. Multiple years of data collected for both low and high annual precipitation years (drought to deluge) are needed to determine long-term effects of management on C (Suyker *et al*., 2003; Verburg *et al*., 2004; Wylie *et al*., 2007). Moreover, quantifying the effect of conservation practices (such as CRP) on growing-season NEE requires methods for scaling-up data collected at a specific site to thousands of fields in production.

While growing-season NEE is highly influenced by climatic variability, environmental drivers alone do not sufficiently explain interannual variability (Hui *et al*., 2003). Biotic factors also significantly influence ecosystem C dynamics, in some cases to a greater degree than abiotic factors (Richardson *et al*., 2007). For example, foliar nitrogen (N) concentration and the amount of LB represent significant sources of annual variability in gross photosynthesis (Field & Mooney, 1986; Walcroft *et al*., 1997), which interact with climate and phenology to alter growing-season NEE (Frank, 2004; Richardson *et al*., 2007). These biotic factors are spatially more variable and more difficult to measure than weather. Satellite and aerial-based methods for quantifying biomass and N content (Phillips *et al*., 2006; Beeri *et al*., 2007b) for grasses in the NGP using Landsat and Advanced Spaceborne Thermal Emission and Reflection Radiometer (ASTER) sensors have expanded the possibilities for including biotic data in C flux models. Both abiotic and remote sensing-based biotic information may explain a large portion of the variance in grassland NEE for a wide range of environmental conditions at landscape scales.

We postulated that growing-season NEE for the 1.3 million ha of ND grasslands enrolled in the CRP in 1996 (1.1 million ha east of the Missouri River and 0.2 million ha west-river) varied over a 10-year contract period. This program compensates producers for planting perennial grasses into fields previously used for annual crop production (USDA, 1997). Management for these 'rested' lands is minimal, with late-summer harvesting permitted only in emergency drought years. Fields under CRP are narrow (often <100 m wide), with contracts extending over 10 years (USDA, 2006). Consequently, coarse-resolution satellite data (e.g. 1000-m pixels) will not resolve individual CRP fields. Determination of cumulative net C uptake on a field-by-field basis over the length of a CRP contract requires modeling multiple years of data with adequate spatial resolution spanning the wide range of climatic variability (drought to deluge) common in the NGP. To the best of our knowledge, remote sensing-based models that assess effects of long-term conservation management on growing-season C uptake across ecoregions have not been published in the NGP or elsewhere. We aimed to determine if annual growing-season net C uptake modeled for 20 620 ha of CRP grasslands located east and west of the Missouri River declined with drought and time since planting over a 10-year contract period.

Methods

Field site for model development

The model development field-site has been consistently managed since 1916 by lightly stocking with cattle (2.6 ha $steer^{-1}$) each year between June and August. Soils at the site are Temvik–Wilton silt loams [FAO: Calcic Siltic Chernozems; USDA: fine-silty, mixed, superactive, frigid Typic and Pachic Haplustolls (Soil Survey, 2006)]. Relative species composition (% basal cover) is 97% grasses and sedges (Beeri *et al*., 2007b). Species include a mixture of blue grama [*Bouteloua gracilis* (H.B.K.) Lag. Ex Griffiths], western wheatgrass [*Pascopyrum smithii* (Rybd) Löve], needle-and-thread [*Hesperostipa comata* (Trin.) and Rupr.], green needle grass [*Nassella viridula* (Trin.) Barkworth], carex (*Carex filifolia* Nutt. and *Carex heliophila* Mack.), smooth brome (*Bromus inermis* Leyss.), and Kentucky bluegrass (*Poa pratensis* L.). Also included are clusters of western snowberry (*Symphoricarpos occidentalis* Hook.) shrubs, which represent 3% of the basal cover. Average annual precipitation (from 1913 to 2006) is 412 mm, with $\sim 65\%$ of the total rainfall during the growing season. Average minimum and maximum temperatures from April to September (1913–2006) are 8.44 and 22.5 °C, respectively. During the study period, annual precipitation ranged from 212 to 571 mm (Mandan Experiment Station, ND).

NEE (g CO_2 m^{-2} h^{-1}) was measured from 1997 to 2006 with a Bowen Ratio Energy-Balance (BREB) instrumentation (Model 023/CO_2 Bowen ratio system, Campbell Scientific Inc., Logan, UT, USA) for a 12.3-ha grassland field-site located at Mandan, ND (46°46′N, 100°55′W) using methods previously described (Dugas *et al*., 1999). The system measures canopy fluxes of CO_2 every 20-min for the entire site, providing net C exchange data at an ecosystem scale. Carbon dioxide

fluxes ($mg\,m^{-2}\,s^{-1}$) were derived by multiplying turbulent diffusivity by the change in the density of CO_2 measured between 1 and 2 m above the canopy and correcting for differences in water vapor density (Webb *et al*., 1980). When turbulent diffusivity estimated by the BREB approach failed, as evidenced by differences in signs of the sensible/latent heat flux calculations and the temperature/water vapor gradient, we calculated turbulent diffusivity using wind speed, atmospheric stability, and canopy height (Dugas *et al*., 1999). This alternative method of estimating diffusivity was used in about 10% of the calculations, which were observed mostly at night. Growing-season NEE ($g\,C\,m^{-2}$ growing season^{-1}) was calculated each year by summing all observations during the growing season (April 15 to September 30). Positive values represent net C uptake. Data collected during rainfall events and instrument malfunction periods were not included. Missing data comprised $<5\%$ of the observations during the growing-season (mostly during rainfall events); gaps in the data were not filled.

Image processing

We used data from two satellite sensors at two spatial resolutions. Landsat data are provided as 30-m pixels, while ASTER data vary with bands and are typically provided as 15- or 30-m pixels. Seventy-one images (65 Landsat and six ASTER) were preprocessed using ERDAS Imagine 8.7 software (Leica Geosystems GIS & Mapping LLC, Norcross, GA, USA). All images were geo-referenced to the same projection (UTM, 14 North, WGS 84 Datum). Landsat digital numbers were converted to ground reflectance (Beeri *et al*., 2007a). We acquired ASTER Level 1B sensor products, with registered radiance at the sensor (Abrams, 2000), on May 19, 2006; June 20, 2006; July 13, 2006; July 22, 2006; August 30, 2006; and September 15, 2006. ASTER images were also calibrated to ground reflectance using the empirical line method on data collected from calibration sites (Moran *et al*., 2001; Clark *et al*., 2002). All image data acquired over the model development field-site were cloud-free. Without *a priori* knowledge of which scenes would be most predictive of growing-season NEE, we used all available Landsat images acquired April–September from 1997 to 2004 and 2006 towards model development (Table 1).

Model development field-site mapping/spectral data calculations

The model development field-site included pixels of the *S. occidentalis* shrubs as well as grasses, which needed to be mapped and modeled separately because net C assimilation rates, biomass, evapotranspiration, leaf chemistry, and optical properties vary strongly between grasses and shrubs (Turner *et al*., 1999; Baldocchi *et al*., 2004; Gao *et al*., 2004). We used a submeter, real-time differential Trimble Geo XT Global Positioning System (GPS) Beacon receiver with an external antenna (Trimble Navigation, Sunnyvale, CA, USA) to geo-locate *S. occidentalis* shrub clusters, which comprised an area of four Landsat pixels (30 m × 30 m). We also used GPS to delineate four representative grass areas (30 m × 30 m) surrounding the BREB system, which were also geo-located to Landsat pixels. This is contrary to methods commonly reported, where a single pixel (Wylie *et al*., 2004; Zhang *et al*., 2007) or a single cluster of pixels (3 pixels × 3 pixels) is selected (Turner *et al*., 1999). In our case, pixels surrounding the BREB system were not 100% grass and required stratification by physiognomic type (Turner *et al*., 1999).

We used spectral algorithms previously developed and validated in NGP ecosystems to estimate biomass and CN for the grass and *S. occidentalis* pixels at the model development field-site (Phillips *et al*., 2006; Beeri *et al*., 2007a). The algorithm used for LB is based on the linear relationship between the Modified Soil-Adjusted Vegetation Index (MSAVI) and biomass field data collected bimonthly during the growing season from 1997 to 2006 for grasses and in 2001 for shrubs (Frank, 2004; Phillips *et al*., 2006). The MSAVI index is computed with Landsat bands 3 (B3) and 4 (B4) as follows:

$$\mathrm{MSAVI} = 0.5 \times ((2 \times \mathrm{B4} + 1) - \sqrt{((2 \times \mathrm{B4} + 1)^2 - 8 \times (\mathrm{B4} - \mathrm{B3}))}). \quad (1)$$

MSAVI index values extracted from grass pixels were used to estimate live grass biomass (LGB) ($kg\,ha^{-1}$) according the following algorithm:

$$\text{Live grass biomass } (kg\,ha^{-1}) = ((\mathrm{MSAVI} - \mathrm{MSAVI}_{\min})/(1 - \mathrm{MSAVI}_{\min})) \times 4671 - 72, \quad (2)$$

where $\mathrm{MSAVI}_{\min}$ was determined by extracting data from a continuously unvegetated sites within each image. Scaling MSAVI reflectance data to a known unvegetated site and normalizing these data relative to a maximum MSAVI reflectance value of 1 is common when comparing multiple images (Qi *et al*., 2000). Similarly, MSAVI index values were extracted from shrub pixels to estimate live shrub biomass (LSB) ($kg\,ha^{-1}$) according the following algorithm:

$$\text{Live shrub biomass } (kg\,ha^{-1}) = ((\mathrm{MSAVI} - \mathrm{MSAVI}_{\min})/(1 - \mathrm{MSAVI}_{\min})) \times 4520 - 48. \quad (3)$$

The spectral algorithm used to estimate canopy CN is based on the linear relationship between the Normalized

Table 1 Landsat imagery processed for use in model development, validation, and application

Date	Sensor	Path-Row	Date	Sensor	Path-Row	Date	Sensor	Path-Row
May 9, 1997	5	033-027	September 1, 2001	7	033-027	September 15, 2003	5	033-027
June 10, 1997	5	033-027	September 26, 2001	7	032-027	May 5, 2004	5	032-027
August 22, 1997	5**	032-027	August 17, 2001	5	032-027	June 6, 2004	5	032-027
September 30, 1997	5	033-027	September 1, 2001	7	033-027	June 29, 2004	5**	033-027
May 12, 1998	5	033-027	September 26, 2001	7	032-027	July 24, 2004	5	032-027
May 28, 1998	5**	033-027	April 13, 2002	7	033-027	September 1, 2004	5	033-027
July 15, 1998	5	033-027	April 29, 2002	7	033-027	September 17, 2004	5	033-027
August 25, 1998	5	032-027	May 15, 2002	7	033-027	April 22, 2005	5	032-027
September 17, 1998	5	033-027	May 31, 2002	7**	033-027	May 15, 2005	5	033-027
April 29, 1999	5	033-027	June 16, 2002	7	033-027	July 2, 2005	5	033-027
July 11, 1999	5**	032-027	June 25, 2002	7	032-027	July 18, 2005	5	033-027
August 19, 1999	5	033-027	July 3, 2002	5	032-027	August 28, 2005	5**	032-027
May 18, 2000	7	032-027	August 3, 2002	7	033-027	September 20, 2005	5	033-027
July 12, 2000	7	033-027	August 19, 2002	7	033-027	April 25, 2006	5	032-027
August 14, 2000	5**	032-027	September 13, 2002	7	032-027	May 27, 2006	5	032-027
September 15, 2000	5	032-027	May 3, 2003	5	032-027	June 3, 2006	5	033-027
April 26, 2001	7	033-027	June 20, 2003	5**	032-027	June 19, 2006	5	033-027
May 12, 2001	7	033-027	July 13, 2003	5	033-027	July 14, 2006	5**	032-027
May 28, 2001	7	033-027	August 7, 2003	5	032-027	August 6, 2006	5	033-027
June 22, 2001	7	032-027	August 14, 2003	5	033-027	August 22, 2006	5	033-027
July 8, 2001	7**	032-027	August 30, 2003	5	033-027	September 7, 2006	5	033-027
August 17, 2001	5	032-027	September 8, 2003	5	032-027			

Scenes acquired from 1997 to 2003 and in 2006 were used in the stepwise regression procedure. Scenes acquired in 2004–2005 were used for accuracy assessment.

**Scenes were used for large-scale model application to Conservation Reserve Program fields in three counties.

Difference of Landsat bands 5 and 3 (ND53) and field data collected bimonthly during the growing season in 2004 and tested in two NGP ecoregions in 2005 (Phillips *et al.*, 2006; Beeri *et al.*, 2007). ND53 is computed from Landsat data as follows to estimate canopy CN:

$$\mathrm{ND53} = (1 - (\mathrm{B5} - \mathrm{B3})/(\mathrm{B5} + \mathrm{B3})), \quad (4)$$

$$\mathrm{CN} = 2.62 + 56.35 \times \mathrm{ND53}, \quad (5)$$

where B3 and B5 are Landsat bands 3 and 5, respectively. Average LB and CN for the four grass and shrub pixels was calculated per date for use in the stepwise regression to estimate growing-season NEE ($\mathrm{g\,C\,m^{-2}}$ growing $\mathrm{season^{-1}}$). Both stepwise regression models were used to calculate the area-weighted NEE for the entire 12.3-ha model development field-site.

Growing-season NEE regression model development and validation

Landsat data acquired from 1997 to 2003 and in 2006 (Table 1) were used to determine the regression model because they represent the greatest range in climatic variability (from deluge to drought) between 1997 and 2006. Landsat imagery collected in 2004 and 2005, along with ASTER data collected in 2006, were reserved for statistical model validation. Stepwise linear regression was performed in SAS (Joyner, 1985) according to Hocking (1976) and selected those variables that significantly ($P < 0.15$) contributed to the variance in growing-season NEE ($\mathrm{g\,C\,m^{-2}\,growing\,season^{-1}}$) for grasses and for *S. occidentalis* shrubs.

Independent input variables for the stepwise regression included: annual precipitation (PPT) from weather stations located east-river at Turtle Lake (47°32′N, 100°53′W) and west-river at the Mandan Experiment Station (46°49′N, 100°54′W), year of image acquisition (YR), image acquisition day of the year (DOY), average LGB or average LSB calculated from the imagery, and average CN calculated from the imagery. We included DOY since imagery from multiple days within a year were evaluated towards developing this model, and we needed to determine if image acquisition date significantly contributed to the variance in growing-season NEE. Actual growing-season NEE, collected from the BREB, was the dependent variable. The final models (1 for grasses, 1 for *S. occidentalis*) were comprised of those variables that significantly affected growing-season NEE measured using the BREB system. These models were used to estimate growing-season NEE

($g\,C\,m^{-2}$ growing season^{-1}) for the entire 12.3-ha model development field-site by weighting the data by area for grass and *S. occidentalis* on each date. We use both regression equations to validate the model in our slightly mixed physiognomy field-site, but we focus on the grass-only equation in subsequent sections of the paper to assess CRP fields planted to perennial grasses. Predicted field-scale growing-season NEE were plotted against actual NEE (measured using the BREB) from 1997 to 2006 using Landsat and for 2006 using ASTER. Model uncertainty was assessed using the regression model R^2 and the root-mean-square-error (RMSE), which was calculated by comparing model-predicted NEE to measured NEE for 18 Landsat and ASTER images reserved for model assessment (Table 1).

Grassland growing-season NEE model application to CRP lands

Growing-season NEE was calculated for fields enrolled in CRP since 1996 for portions of McLean, Oliver and Morton counties, ND (USDA, 2006). A total of 1434 CRP fields within these counties were located within one Landsat scene (Fig. 1). McLean county fields (1272 total) are located on the east side of the Missouri River in the Northern Glaciated Plains ecoregion (Omernik, 1987). Oliver and Morton fields (165 total) are located on the west side of the Missouri River in the NGP ecoregion. Dominant soil series for CRP fields both east and west-river are Pachic or Typic Haplustolls (Soil Survey, 2006), which are similar to soils at the model development field-site. CRP fields on both sides of the river are dominated by *B. inermis* and crested wheatgrass [*Agropyron desertorum* (Fisch. ex Link) J.A. Schultes], with some fields intermixed with intermediate wheatgrass [*Thinopyrum intermedium* (Host) Barkworth & D.R. Dewey] and alfalfa (*Medicago* L.). Annual precipitation data were collected east-river from a weather station at Turtle Lake, and west-river from a weather station at Mandan (http://cdo.ncdc.noaa.gov/CDO/cdo). Growing-season NEE was determined using the grassland regression model on Landsat images acquired during peak growing season from 1997 to 2006 (Table 1) in ERDAS Imagine. Clouds were masked by filtering bands 2–6 several times (Irish, 2000) and then processed manually (Beeri & Phillips, 2007a); cloud-pixels were omitted from additional analyses. Clouds comprised <1% of the dataset from 2000 to 2006, and <3% of the dataset from 1997 to 1999. Average growing-season NEE, GLB, and CN for each year was calculated by CRP field. Then, average growing season NEE, GLB and CN was calculated for all CRP fields east (1200 fields total) and west (300 fields total) of the Missouri River. Nitrogen content ($mg\,g^{-1}$) was estimated from CN data, using a constant ($400\,mg\,g^{-1}$) for perennial grass carbon content (Beeri *et al.*, 2007b). Average growing-season

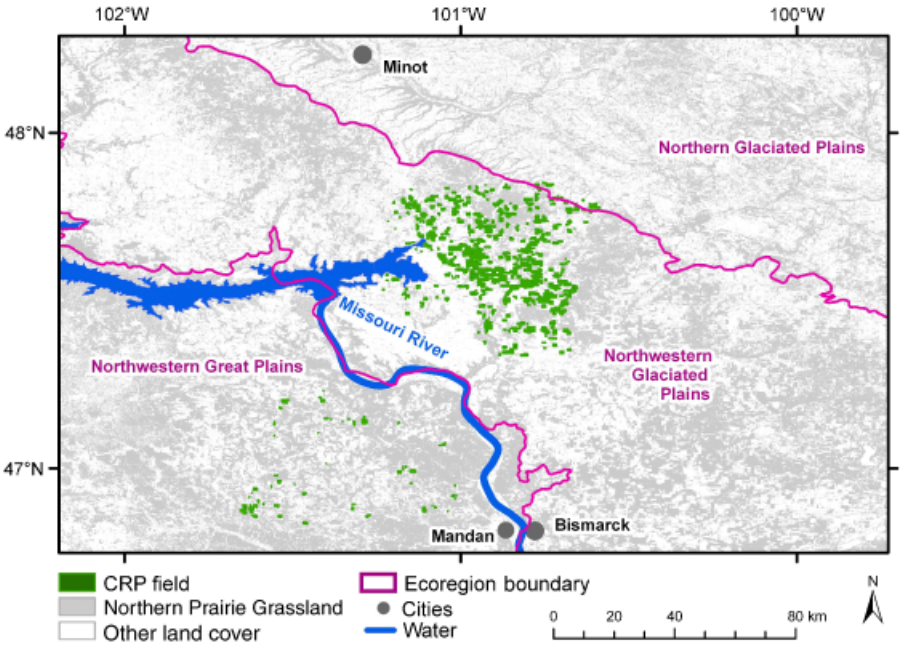

Fig. 1 Map of perennial grass fields enrolled in Conservation Reserve Program (CRP) and located within the satellite images acquired from 1997–2006 for McLean, Morton, and Oliver counties, ND. We located 1272 fields (19 310 ha) east of the Missouri River (McLean) within the Northwestern Glaciated Plains ecoregion and 165 fields (1310 ha) west of the Missouri River (Morton and Oliver) within the Northwestern Great Plains ecoregion. Total number of hectares mapped here represent <2% of the total North Dakota area now enrolled in CRP.

NEE by field was summed for all years to determine the overall average 10-year cumulative growing-season NEE for CRP fields east-river vs. west-river.

Results and discussion

Modeled growing-season NEE based on the Mandan Field-Site

Results of the stepwise regression for both grasses and shrubs indicated that LB (LGB or LSB), CN, YR, and PPT all significantly ($P<0.15$) contributed to the statistical model, with a model R^2 of 0.89 for grasses and 0.76 for shrubs. DOY also significantly contributed to the growing-season NEE variance for grasses (Tables 2 and 3). Coefficients for each variable were derived from the stepwise regressions to form the following equations:

$$\begin{aligned}\text{Grass NEE } (\text{g C m}^{-2}\,\text{growing season}^{-1}) &= (\text{LGB} \times 0.2745) + (\text{CN} \times 30.66) + (\text{DOY} \times 0.5139) \\ &\quad + (\text{PPT} \times 0.9785) - (\text{YR} \times 93.31) - 844,\end{aligned} \tag{6}$$

$$\begin{aligned}\text{Shrub NEE } (\text{g C m}^{-2}\,\text{growing season}^{-1}) &= (\text{LSB} \times 0.1306) + (\text{CN} \times 17.18) \\ &\quad + (\text{YR} \times 33.11) + (\text{PPT} \times 0.9379) - 506.16.\end{aligned} \tag{7}$$

Table 2 Summary of stepwise selection for grassland growing-season net ecosystem exchange

Step	Variable	Partial R^2	Model R^2	C (p)	F value	Pr > F
1	YR	0.6374	0.6374	458.847	376.17	<0.0001
2	PPT	0.0944	0.7318	286.155	75.00	<0.0001
3	CN	0.0501	0.7819	195.549	48.65	<0.0001
4	LGB	0.1006	0.8825	11.4685	180.55	<0.0001
5	DOY	0.0038	0.8862	6.4527	7.00	<0.0088

YR, year of image acquisition; PPT, annual precipitation; CN, carbon : nitrogen ratio; LGB, live grass biomass; DOY, day of the year.

Table 3 Summary of stepwise selection for *Symphoricarpos occidentalis* growing-season net ecosystem exchange

Step	Variable	Partial R^2	Model R^2	C (p)	F value	Pr > F
1	PPT	0.6530	0.6530	8.7699	62.10	<0.0001
2	CN	0.0048	0.6878	6.7791	3.57	<0.0679
3	YR	0.0203	0.7381	5.0174	2.33	<0.1374
4	LSB	0.0261	0.7642	4.0251	3.21	<0.0836

PPT, annual precipitation; CN, carbon : nitrogen ratio; LSB, live shrub biomass; DOY, day of the year.

Previous work with grasslands in the NGP has shown that NEE covaries strongly with precipitation, LB, and plant nitrogen. Carbon uptake for grasses also varies with DOY because leaf area and net C assimilation tends to track climatic conditions during the growing season (Frank, 2004; Xu & Baldocchi, 2004). *S. occidentalis* growing-season NEE was not significantly affected by DOY because leaf area and net C assimilation for *S. occidentalis* is less variable during the growing season than for grasses (Baldocchi *et al*., 2004; Gao *et al*., 2004; Xu & Baldocchi, 2004).

Area-weighted growing-season NEE, calculated from all images over the entire 12.3-ha model development field-site and averaged by year, compared reasonably well with measured growing-season NEE (Fig. 2). Error bars for Fig. 2 indicate the range of growing-season NEE values determined on different dates within a year (Table 1). The slope of the regression line for measured vs. estimated NEE across all years indicated a near one-to-one correspondence (slope = 0.90) with a y-intercept of 1.54. Across years, images acquired in April (when LB was lowest) were the least predictive whereas data acquired in mid-summer most closely tracked measured growing-season NEE.

Our Landsat-based estimates of NEE for the model development field-site are comprised of 136 pixels of information, area-weighted by the proportion of grass and *S. occidentalis* physiognomic types. Our ASTER-based estimates of NEE for the model development

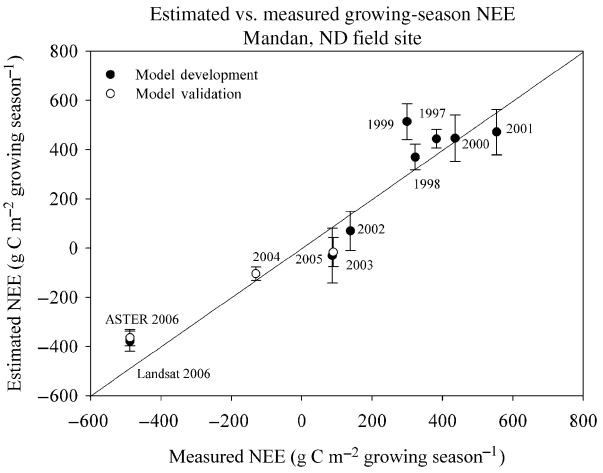

Fig. 2 Estimated vs. measured growing-season net ecosystem exchange (NEE) by year, based on data from 71 satellite images collected between April and September 1997–2006. All images were acquired from the Landsat sensors, with the exception of 2006. During 2006, growing-season NEE was also estimated separately using data from six ASTER scenes. Error bars indicate the range of data estimated using multiple images acquired within a growing season (Table 1).

field-site are comprised of 546 pixels of information also area-weighted by physiognomic type. The RMSE, calculated using the 2004–2005 Landsat data (12 images) and 2006 ASTER data (six images), was 270 g C m^{-2} growing season^{-1}. Model accuracy assessment methodology reported here follows Kokaly & Clark (1999), where the regression equations developed from a calibration subset of data (53 images) were used to predict growing-season NEE for the remaining validation dataset (18 images). Others have instead used cross-validation to assess accuracy of predicted NEE using 1000-m pixels collected daily and composited over 10 days with <0.2 relative error (Wylie *et al.*, 2007). In this case, model development and field-site validation were based on one pixel of information in space (instead of 136 or 546 pixels) across six unique NGP grassland sites every 10 days. Our approach, using Landsat and ASTER, was to provide intensive measurements of spatial variability for one site only to support questions more specific to small (<10 ha) ND fields enrolled in CRP. Differences among reported RMSEs underscore the importance of methodology, pixel size selection, temporal resolution, and the range of spatial variability delineated when comparing remote sensing-based NEE models.

Growing-season NEE for grasses in CRP

Our dataset included 19 310 ha of CRP land east-river and 1310 ha west-river, with average field sizes of 15.3 and 7.0 ha, respectively. Average growing-season NEE for CRP fields east-river (n = 1272) ranged from −211 in 2006 to 634 g C m^{-2} growing season^{-1} in 2000. Average growing-season NEE for CRP fields west-river (n = 165) ranged from −366 g C m^{-2} growing season^{-1} in 2006 to 692 g C m^{-2} growing season^{-1} in 1999 (Fig. 3). Since data for both sides of the river were collected from the same image, year-to-year differences in growing-season NEE were due to observed difference in LB, CN, and PPT (Table 4). Divergence in annual means between CRP fields on opposite sides of the Missouri River (Fig. 3)

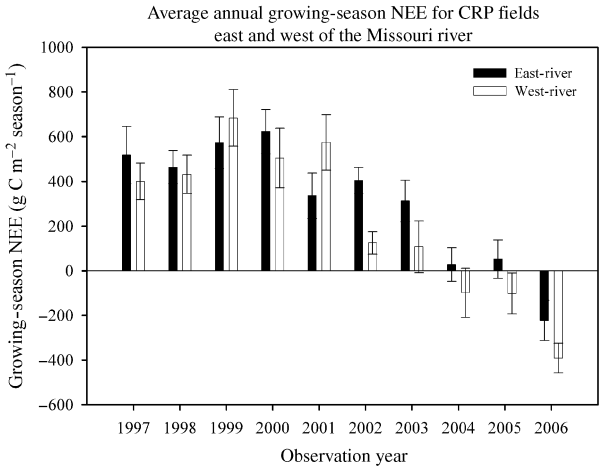

Fig. 3 Average growing-season net ecosystem exchange (NEE) estimated by Conservation Reserve Program (CRP) field for each year on opposites sides of the Missouri River. A total of 1272 CRP fields were observed east-river and 165 CRP fields were observed west-river within the same Landsat image on 65 days between April and September, 1997–2006 (Table 1). Error bars represent the standard deviation of growing-season NEE for each group of fields located east- and west-river.

Table 4 Average (± std. dev.) canopy carbon : nitrogen ratio (CN), live biomass, annual precipitation, and estimated N content observed each growing season from 1997 to 2006 for all Conservation Reserve Program fields in the dataset located east and west of the Missouri River

	East-river				West-river			
Year	CN	LB (kg ha^{-1})	PPT (mm)	N (mg g^{-1})	CN	Live biomass (kg ha^{-1})	PPT (mm)	N (mg g^{-1})
1997	23.7 (3.7)	759 (328)	425	16.9	19.3 (10.2)	397 (314)	345	20.7
1998	21.1 (3.2)	828 (410)	557	19.0	20.8 (2.8)	860 (385)	524	19.2
1999	20.7 (2.9)	1414 (460)	599	19.3	20.5 (2.1)	1924 (501)	571	19.5
2000	27.6 (2.3)	976 (263)	634	14.5	26.4 (2.4)	1139 (407)	492	15.2
2001	24.5 (2.6)	1770 (440)	329	16.3	24.2 (3.2)	1971 (618)	534	16.5
2002	35.5 (1.7)	465 (160)	526	11.3	34.9 (1.9)	548 (174)	228	11.5
2003	26.6 (1.9)	1611 (433)	482	15.0	25.7 (2.0)	1940 (539)	212	15.6
2004	26.2 (1.9)	1253 (363)	396	15.3	26.3 (1.7)	1079 (415)	339	15.2
2005	28.6 (2.2)	823 (265)	534	14.0	28.7 (2.0)	673 (282)	431	13.9
2006	29.5 (1.5)	815 (296)	347	13.6	31.9 (1.2)	431 (207)	220	12.5

Included are 1272 fields in McLean (east-river) and 165 fields in Morton and Oliver counties (west-river).

was primarily driven by differences in PPT from 2002 to 2006 (Table 4). For four of these 5 years, PPT west-river was only 50–65% of the long-term average (412 mm). Continuously dry spring conditions during these years resulted in very low and often negative values for growing-season NEE (Fig. 3). Annual precipitation east-river remained near or above the 30-year average (440 mm). The exceptions were in 2001 and 2006, when precipitation dropped to 10–20% below average (Table 4), primarily due to low snowfall. Sharp declines in snowfall from 2001 to 2006 reduced surface waters in central ND by 50% (Beeri & Phillips, 2007a) and may have been associated with lower growing-season NEE in these years. However, the direct effect of snowfall on NEE in the NGP needs quantification.

Average N content ranged from a high of 20.7 mg g^{-1} in 1996 to a low of 11.3 mg g^{-1} in 2002, with a general decline in canopy N from 1996 to 2006 on both sides of the river (Table 4). Declines in canopy N towards the end of the 10-year time series could be attributed to (a) depletion of residual nutrients available following conversion from annual to perennial grasses and (b) the accumulation of nonphotosynthetically active plant material. Before CRP enrollment, these fields were intensively managed for crop production, with nutrients annually applied according to agronomic recommendations. Residual nutrients following years of regular fertilization were likely mined by the deeper, more pervasive perennial grass rooting systems. Also, photosynthetically active radiation likely penetrated the newly planted grass canopy more easily during the initial years of CRP establishment. Closure of the canopy over time by nonphotosynthetically active material would reduce canopy N, which often comprises $>50\%$ of the total biomass in NGP grasslands (Beeri *et al*., 2007b). This increase in nonphotosynthetically active plant material and depletion of soil nutrients following conversion from annual cropping to CRP likely contributed to declines in canopy N several years following perennial grass establishment.

Cumulative growing-season NEE, or the sum of NEE by CRP field from 1997 to 2006, was 3170 g C m^{-2} east-river and 2380 g C m^{-2} west-river (Fig. 4). The 19 310 ha of CRP land evaluated east-river removed 612 100 metric tons of atmospheric CO_2–C from 1997 to 2006. The 1310 ha of CRP land evaluated west-river removed 31 200 metric tons of atmospheric C from 1997 to 2006. These data, while useful for county or ecoregion-scale comparisons of C uptake for CRP lands during the growing season, do not account for C losses during the dormant period (October 1 to April 14). Senescent material is also not accounted for, since spectral data necessary to separate senescent from live vegetation is not acquired by the Landsat sensor (Beeri *et al*., 2007b).

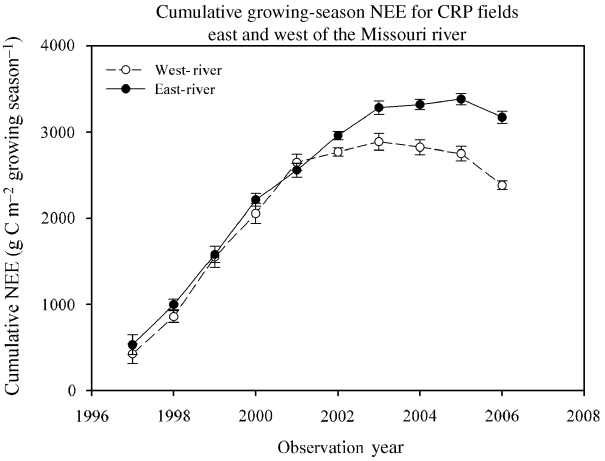

Fig. 4 Cumulative growing-season net ecosystem exchange (NEE), based on the sum of annual averages for Conservation Reserve Program (CRP) fields east and west-river (see Fig. 3). Data were acquired on the same day for CRP field both east and west of the Missouri River using the Landsat sensors (Table 1). Error bars represent the standard deviation of cumulative growing-season NEE for each group of fields located east- and west-river.

Dormant-season respiratory losses will ultimately determine annual net C gains or losses (Valentini *et al*., 2000) and have been shown to offset C gains by 70% (Frank, 2004). Consequently, these data must be considered carefully, with the understanding that annual NEE will be significantly lower than growing-season NEE. Additional work should include spatially explicit models (Richardson *et al*., 2006) for estimating field and landscape scale dormant-season NEE in ND grasslands. Future applications of satellite-based surface temperature data may assist with modeling some of the variance in dormant-season respiration for specific sites in conjunction with process-level modeling (Richardson *et al*., 2006).

Our validation included data acquired from two multispectral satellite sensors, where we used spectra in the red, near-infrared (NIR), and shortwave infrared (SWIR) bands. Specific bandwidths in the NIR and SWIR are different between sensors, with narrower bands of information from ASTER (NIR 760–860 nm; SWIR 1600–1700 nm) compared with Landsat (NIR 760-900; SWIR 1550-1750). Agreement between the ASTER and Landsat-based estimates for 2006 (Fig. 2) suggest data from other moderate-to-high resolution multispectral sensors might also provide data which significantly affect growing-season NEE. Other high-resolution satellite sensors equipped with red, NIR and SWIR spectral information include the China–Brazil Earth Resource Satellite (CBERS), the Indian Remote Sensing Satellite (IRS), and

the Satellite Pour l'Observation de la Terre (SPOT). These provide data as 20-m, 23.5-m, and 10-m pixels, respectively, and could be evaluated similarly.

We report results for central ND grasslands under CRP only; however, these methods could be applied to other grasslands located near sites where C flux data are continuously collected. Given the satellite-data archive and networks of C flux information, other grassland systems with varying climatic regimes could also be analyzed retrospectively in a similar manner using other multispectral sensors. With NEE information necessary for model calibration, these types of moderate-to-high resolution data-driven models could help to answer how management may have affected C fluxes on a field-by-field basis. Further, these higher spatial resolution data could then be fused with coarser scale spatial resolution products to build a data hierarchy capable of addressing questions at multiple scales. Building multispectral data-based models potentially applicable to more than one satellite sensor expands application options and reduces the risk of relying on one satellite to drive all models for growing-season NEE.

Conclusions

Global change questions, including how land-use influences ecosystem C fluxes, require scaling up site-specific knowledge using the best available science and technology. Ideally, multiple sensors would be employed to effectively address questions at varying scales—from fields to landscapes to regions. We used 8-years of Landsat and field data in a stepwise linear regression procedure to create a model for estimating grassland growing-season NEE at field and landscape scales, where year, LB, CN ratio, annual precipitation, and DOY explained 89% of the variability. We used three additional years of Landsat, ASTER, and field data to validate the model. Our model for growing-season NEE is based on weather and satellite-based data acquired only during the growing season and does not include dormant season fluxes. Observed growing-season NEE from 1997 to 2006 vacillated with drought and deluge, with net C losses to the atmosphere in 2006.

We estimated cumulative NEE for small crop fields converted from annual crops to conservation reserve perennial grasses over 10 growing seasons. Landsat-based observations on 65 dates for counties east and west of the Missouri River were used to estimate growing-season NEE and evaluate spatial variability. We found cumulative growing-season NEE for fields west-river diverged distinctively from fields east-river during the 2002–2006 time-period, which corresponded an overall 30% reduction in annual rainfall. West-river, cumulative growing-season NEE from 2002 to 2006 was 25% lower than for fields located east-river, where precipitation more closely tracked the long-term average.

Results reported here represent the first, to the best of our knowledge, large-scale assessment of C uptake for fields under the CRP. We observed 20 620 ha of perennial grass fields and found they removed a total of 643 300 metric tons of atmospheric C over 10 growing seasons. The area observed here represents $<2\%$ of ND's total CRP enrollment, where currently 1.1 million ha are located east-river and 0.2 million ha are located west-river (USDA, 2006). Based on average cumulative growing-season NEE estimated for fields east- ($3170\,g\,C\,m^{-2}$) and west-river ($2380\,g\,C\,m^{-2}$), 35.9 and 4.8 Tg of C may have been removed during 10 growing seasons by perennial grasses planted east and west of the Missouri River, respectively, while enrolled in CRP. Spatially explicit dormant season fluxes, which are needed to report total annual NEE, are not included in these estimates and should be the focus of future research.

Acknowledgements

We sincerely thank Al Frank for his generous support of this project and Scott Bylin for data collection and processing. We also thank ARS scientists Jon Hanson, Jack Morgan, Mark Liebig, Dave Archer, Bruce Wylie (EROS Data Center), Susan Samson-Liebig (NRCS), Ryan Powers (USDA-APHIS), and Darin Blunck (Ducks Unlimited) for their thoughtful reviews and suggestions. Special thanks to Leon Maldonado Jr at the Jet Propulsion Laboratory for his assistance targeting the ASTER scenes. This work represents a collaborative effort by the ARS, NRCS and Farm Services Agencies and was supported by the USDA Cooperative Agreement 58-5445-7-319 and the Rangeland, Livestock, and Integrated Agriculture National Programs.

References

Abrams M (2000) The Advanced Spaceborne Thermal Emission and Reflection Radiometer (ASTER): data products for the high spatial resolution imager on NASA's Terra platform. *International Journal of Remote Sensing*, **21**, 847–859.

Baldocchi DD, Xu L, Kiang N (2004) How plant functional-type, weather, seasonal drought, and soil physical properties alter water and energy fluxes of an oak-grass savanna and an annual grassland. *Agricultural and Forest Meteorology*, **123**, 13–39.

Beeri O, Phillips RL (2007a) Tracking palustrine water seasonal and annual variability in agricultural wetland landscapes using Landsat from 1997 to 2005. *Global Change Biology*, **13**, 897–920.

Beeri O, Phillips RL, Hendrickson J, Kronberg S (2007b) Estimating forage quantity and quality using aerial hyperspectral imagery for northern mixed grass prairie. *Remote Sensing of Environment*, **110**, 216–225.

Clark RN, Swayze GA, Livo KE *et al.* (2002) Surface reflectance calibration of terrestrial imaging spectroscopy data: a tutorial using AVIRIS. In: *Proceedings of the 10th Airborne Earth Science*

Workshop, JPL Publication 02-I (ed. Green RO), pp. 1–21. Pasadena, California.

Dugas WA, Heuer H, Mayeux HS (1999) Carbon dioxide fluxes over bermudagrass, native prairie, and sorghum. *Agricultural and Forest Meteorology*, **93**, 121–139.

Field C, Mooney HA (1986) The photosynthesis–nitrogen relationship in wild plants. In: *On the Economy of Plant Form and Function* (ed. Givnish TJ), pp. 22–55. Cambridge University Press, Cambridge.

Frank AB (2004) Six years of CO_2 flux measurements for a moderately grazed mixed-grass prairie. *Environmental Management*, **33**, S426–S431.

Gao Q, Zhang X, Huang Y, Xu H (2004) A comparative analysis of four models of photosynthesis for 11 plant species in the Loess Plateau. *Agricultural and Forest Meteorology*, **126**, 203–222.

Hocking RR (1976) The analysis and selection of variables in a linear regression. *Biometrics*, **32**, 1–50.

Hui D, Luo Y, Katul G (2003) Partitioning interannual variability in net ecosystem exchange between climatic variability and functional change. *Tree Physiology*, **23**, 433–442.

Irish RR (2000) Landsat 7 automatic cloud cover assessment. In: *Proceedings of Algorithms for Multispectral, Hyperspectral, and Ultraspectral Imagery VI* (eds Sylvia SS, Michael RD), pp. 348–355. The International Society of Optical Engineering, Orlando, FL.

Joyner SP (1985) *SAS User's Guide: Statistics, version 5*. SAS Institute, Cary.

Knapp AK, Fay PA, Blair JM *et al.* (2002) Rainfall variability, carbon cycling, and plant species diversity in a mesic grassland. *Science*, **298**, 2202–2205.

Kokaly RF, Clark RN (1999) Spectroscopic determination of leaf biochemistry using band depth analysis of absorption features and stepwise linear regression. *Remote Sensing of Environment*, **67**, 267–287.

Moran MS, Bryant R, Thome K *et al*. (2001) A refined empirical line approach for reflectance factor retrieval from Landsat 5 TM and Landsat 7 ETM +. *Remote Sensing of Environment*, **78**, 71–82.

Omernik JM (1987) Ecoregions of the conterminous United States. *Annals of the Association of American Geographers*, **77**, 118–125.

Phillips RL, Beeri O, Liebig M (2006) Landscape estimation of canopy C/N ratios under variable drought stress in Northern Great Plains rangelands. *Journal of Geophysical Research*, **111**, G02015.

Qi J, Marsett RC, Moran MS *et al*. (2000) Spatial and temporal dynamic of vegetation in the San Pedro River basin area. *Agriculture and Forest Meteorology*, **105**, 55–68.

Richardson AD, Hollinger DY, Aber JD *et al*. (2006) Comparing simple respiration models for eddy flux and dynamic chamber data. *Agricultural and Forest Meteorology*, **141**, 219–234.

Richardson AD, Hollinger DY, Aber JD, Ollinger SV, Braswell BH (2007) Environmental variation is directly responsible for short- but not long-term variation in forest-atmosphere carbon exchange. *Global Change Biology*, **13**, 788–803.

Robertson GP, Paul EA, Harwood RR (2000) Greenhouse gases in intensive agriculture: contributions of individual gases to the radiative forcing in the atmosphere. *Science*, **289**, 1922–1925.

Rogler GA, Haas HJ (1946) Range production as related to soil moisture and precipitation on the Northern Great Plains. *Journal of the American Society of Agronomy*, **38**, 378–389.

Soil Survey Staff, Natural Resources Conservation Service, United States Department of Agriculture. Soil survey of McLean, Morton and Oliver County Areas, North Dakota [Online WWW]. Available URL: http://soildatamart.nrcs.usda.gov/County.aspx?State=ND [Accessed 7 January 2006].

Suyker AE, Verma SB, Burba GG (2003) Interannual variability in net CO_2 exchange of a native tallgrass prairie. *Global Change Biology*, **9**, 255–365.

Turner DP, Cohen WB, Kennedy RE, Fassnacht KS, Briggs JM (1999) Relationships between leaf area index and Landsat TM spectral vegetation indices across three temperate zone sites. *Remote Sensing of Environment*, **70**, 52–68.

USDA (1997) Conservation Reserve Program (CRP) Final Rule 7 CFR Parts 704 and 1410, US Federal Register v62 no. 3, pp. 7601–7635.

USDA (2006) Conservation Reserve Program Summary and Enrollment Statistics (ed. Barbarika A), Farm Services Agency, Washington, DC.

Valentini R, Matteucci G, Dolman AJ *et al*. (2000) Respiration as the main determinant of carbon balance in European forests. *Nature*, **404**, 861–865.

Verburg PS, Arnone JAI, Obrist D *et al*. (2004) Net ecosystem carbon exchange in two experimental grassland ecosystems. *Global Change Biology*, **10**, 498–508.

Walcroft SS, Whitehead D, Silvester WB, Kelliher FM (1997) The response of photosynthetic model parameters to temperature and nitrogen concentration in *Pinus radiata* D. Don. *Plant, Cell and Environment*, **20**, 1338–1348.

Webb EK, Pearman GI, Leuning R (1980) Correction of flux measurements for density effects due to heat and water vapour transfer. *Quarterly Journal of Royal Meteorological Society*, **106**, 85–100.

Wylie BK, Fosnight EA, Gilmanov TG, Frank AB, Morgan JA, Haferkamp MR, Meyers TP (2007) Adaptive data-driven models for estimating carbon fluxes in the Northern Great Plains. *Remote Sensing of Environment*, **106**, 399–413.

Wylie BK, Gilmanov TG, Johnson DA *et al*. (2004) Intra-seasonal mapping of CO_2 flux in rangelands of northern Kazakhstan at one-kilometer resolution. *Environmental Management*, **33**, S482–S491.

Xu L, Baldocchi DD (2004) Seasonal variation in carbon dioxide exchange over a Mediterranean annual grassland in California. *Agricultural and Forest Meteorology*, **1232**, 79–96.

Zhang L, Wylie BK, Loveland T, Fosnight E, Tieszen LL, Ji L, Gilmanov TG (2007) Evaluation and comparison of gross primary production estimates for the Northern Great Plains grasslands. *Remote Sensing of Environment*, **106**, 173–189.

